1 Corresponding author: V.V. Atuchin

2 Institute of Semiconductor Physics, Novosibirsk 630090, Russia

3 Phone: +7 (383) 3308889

4 E-mail: atuchin@isp.nsc.ru

5

6

New candidate to reach Shockley–Queisser limit: the DFT study of

orthorhombic silicon allotrope Si(oP32)

A.S. Oreshonkov[1,2], E.M. Roginskii, [3] V.V. Atuchin[4,5,6]

[1]Laboratory of Molecular Spectroscopy, Kirensky Institute of Physics Federal Research Center

KSC SB RAS, Krasnoyarsk 660036, Russia

[2]Siberian Federal University, Krasnoyarsk 660041, Russia

[3]Laboratory of Spectroscopy of Solid State, Ioffe Institute, St. Petersburg 194021, Russia

[4]Laboratory of Optical Materials and Structures, Institute of Semiconductor Physics, SB RAS,

Novosibirsk 630090, Russia

[5]Functional Electronics Laboratory, Tomsk State University, Tomsk 634050, Russia

[6]Research and Development Department, Kemerovo State University, Kemerovo 650000, Russia

18

19 **Abstract**

20 In the present study, the unit cell parameters and atomic coordinates were predicted for the *Pbcm*

21 orthorhombic structure of Si(oP32) modification. This new allotrope of silicon is mechanically

22 stable and stable with respect to the phonon states. The electronic structure of Si(oP32) is calculated

23 for LDA and HSE06 optimized structures. The band gap value E_g = 1.361 eV predicted for

24 Si(oP32) is extremely close to the Shockley–Queisser limit and it indicates that the Si(oP32)

25 modification is a promising material for efficient solar cells. The frequencies of Raman and Infrared

26 active vibrations have been calculated for allotrope Si(oP32).

27 **Keywords:** Silicon, allotrope, Shockley–Queisser limit, DFT, phonon

1. Introduction

The diamond-like cubic silicon (Fig. 1) is a semiconductor with the indirect band gap equal to 1.12 eV [1,2]. This elemental material is abundant in nature and, due to its appropriate combination of structural, chemical, mechanical and electronic properties, is widely used in modern electronics, solar cells and chemical industry. Commonly, only the Si allotropes with amorphous and diamond-like structures are widely known as stable in ambient conditions. In the recent decades, the search for new allotropes of Si has attracted considerable attention because most of chemical and physical properties depend on the crystal structure, and it is reasonably expected that new crystal structures might result in novel properties. As a result, many new thermodynamically stable silicon structures were predicted and their properties were theoretically observed [3-11] including the cases when the common tetragonal coordination of Si atoms transform into other forms [3,4,8]. Besides theoretical investigations, the experimental studies were implemented with the use of different preparation routes and several Si allotropes were synthesized to observe their structural and physical characteristics [12-14].
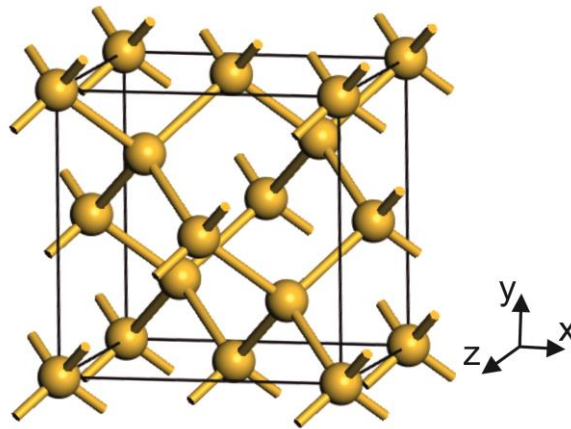
Fig. 1. Crystal structures of cubic silicon

Recently, new germanium allotrope Ge(oP32) with the structure in space group *Pbcm* has been synthesized by the mild-oxidation/delithiation of Li_7Ge_{12} in ionic liquids [15]. The powder and single crystal products were obtained by the reaction at 135-145 ℃ for several days. It is particularly interesting that Ge(oP32) crystals are stable in ambient conditions. The allotrope has as low direct optical band gap as $E_g = 0.33$ eV and is stable up to 363 °C. Thus, the transformation

1   from the diamond-like to orthorhombic structure results in a drastic band gap energy variation. As

2   for silicon, to the best of our knowledge, the related allotrope Si(oP32) has not been considered up

3   to now and its stability and properties remain unknown. Hence, the present study is aimed at the *ab

4   initio* calculations to evaluate the structure and physical properties of silicon allotrope Si(oP32)

5   isostructural to orthorhombic Ge(oP32).

6   **2. Calculations**

7   All the structural optimization, energy and vibrational calculation were carried out by the

8   CASTEP code using the density-functional theory [16]. The structure of orthorhombic Ge(oP32)

9   with the *Pbcm* space group was taken as the initial basis and the germanium atoms were replaced by

10 silicon ones [15]. This structure was fully optimized using the local density approximation (LDA)

11 provided by the Perdew and Zunger [17] parameterization of the numerical results of Ceperley and

12 Alder (CA-PZ) [18] and using the nonlocal exchange-correlation HSE06 functional [19].

13 The calculations of both cubic diamond-like and orthorhombic *Pbcm* structures were

14 performed using the norm-conserving pseudopotential with $3s^2\ 3p^2$ electrons for Si atoms treated as

15 valence ones. The self-consistent field (SCF) procedure was used with a convergence threshold of

16 $5.0 \cdot 10^{-8}$ eV/atom. The total energy was corrected for the finite basis set with 3 cut-off energies. The

17 geometry optimizations were performed at the convergence threshold of 0.001 eV Å^{-1} on the max

18 force, 0.01 GPa - on the max stress. The energy cutoff was set to be 900 eV, and the Brillouin zone

19 (BZ) was sampled by 4×3×4 and 6×6×6 k-points using the Monkhorst–Pack scheme [20] for

20 orthorhombic and cubic structures, respectively. The electronic band structure was calculated within

21 the hybrid functional HSE06 method [16] as for the structure obtained after the geometry

22 optimization, using HSE06 as for the LDA relaxed structure. The phonon spectra at the Γ-point of

23 the BZ and Raman tensor components were calculated within the density functional perturbation

24 theory and the finite displacement method [21, 22] based on the crystal system type. The Raman

25 spectra were simulated by the Lorentzian distribution with a fixed HWHM equal to 2 cm^{-1}. The

26 dispersion of phonon branches along high symmetry directions of the Brillouin zone was calculated

27 using the linear response method [23].

1   Quasiparticle *GW* calculations [24] were performed using the ABINIT code [25,26]. The

2   one-shot G_0W_0 quasiparticle energies were computed using the Kohn-Sham eigenstates and

3   eigenvalues calculated within the LDA approximation as the initial solution of non-interacting

4   Hamiltonian. The inverse dielectric matrix $\epsilon_{GG'}^{-1}(q,\omega)$ was calculated by the random phase

5   approximation (RPA) using 192 unoccupied bands. The dynamic screening was calculated using the

6   contour deformation method [27]. The wavefunctions with maximal kinetic energy 35 Ha were used

7   in the calculations. The corrections to Kohn-Sham energies were calculated as $\Sigma - E_{xc}$ operator

8   diagonal matrix elements, where $\Sigma = GW$ - self-energy operator, E_{xc} - exchange-correlation energy

9   operator, G - Green function, and $W = \epsilon^{-1}v$ - screening Coulomb interaction operator. The

10   components of wavefunction with energies below 750 eV for both exchange and correlation parts

11   were used to calculate Σ.

12   **3. Results and discussion**

13   The optimized crystal structure of Si(oP32) is shown in Figure 2 and the obtained

14   crystallographic data are summarized in Table 1. The difference between the calculated unit cell

15   parameters using LDA and HSE06 does not exceed 0.016 Å. The obtained fractional coordinates

16   differ only in the third decimal place.
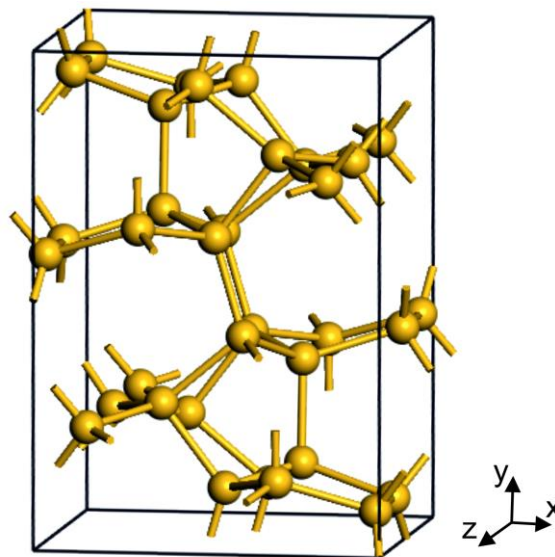
17

18   Fig. 2. Crystal structures of predicted silicon allotrope Si(oP32).

4

Table 1. The calculated structural parameters and atomic positions of Si(oP32), as obtained by LDA and HSE06 (shown in parentheses)

		Unit cell parameters		
	a, Å	*b*, Å	*c*, Å	
	7.777625	11.194104	7.387129	
	(7.785639)	(11.186565)	(7.402904)	

Atom	Wyckoff site	Fractional atomic coordinates		
Si1	4d	0.56517	0.08464	0.25000
		(0.56592)	(0.08406)	(0.25000)
Si2	4d	0.33135	0.22142	0.25000
		(0.33106)	(0.22017)	(0.25000)
Si3	4d	0.48543	-0.11273	0.25000
		(0.48599)	(-0.11346)	(0.25000)
Si4	8e	-0.02380	0.41322	0.08613
		-0.02378	(0.41340)	(0.08639)
Si5	4c	0.15389	0.25000	0.00000
		(0.15405)	(0.25000)	(0.00000)
Si6	8e	0.69943	0.14703	-0.01212
		(0.69939)	(0.14682)	(-0.01221)

The mandatory part of mechanical stability of a crystal lattice is the calculations of elastic constants and elastic moduli [28, 29]. The elastic behavior of a lattice is described by the second-order elastic constant matrix C_{ij} [30]. The calculated stiffness matrix C_{ij} of orthorhombic *Pbcm* silicon is presented below.

$$C_{ij}=\begin{pmatrix} 146.07 & 45.46 & 51.31 & & & \\ 45.46 & 154.12 & 39.23 & & & \\ 51.31 & 39.23 & 181.75 & & & \\ & & & 44.18 & & \\ & & & & 55.08 & \\ & & & & & 45.76 \end{pmatrix}$$

The *necessary* and *sufficient* Born criteria for an orthorhombic system stability [30] are $C_{11}>0$, $C_{11}C_{22}>C_{12}^2$, $C_{11}C_{22}C_{33}+2C_{12}C_{13}C_{23} - C_{11}C_{23}^2 - C_{22}C_{13}^2 - C_{33}C_{12}^2>0$, $C_{44}>0, C_{55}>0$, $C_{66}>0$. All the above conditions are satisfied for the predicted orthorhombic structure. Thus, the predicted structure of Si(oP32) allotrope is stable with respect to elastic properties. The calculated bulk modulus (*B*) value is found to be equal to 83.19 GPa. The results obtained in this work for cubic

1 silicon: B=98.00 GPa and C_{11}=163.97 GPa, C_{12}=65.02 GPa, C_{44}=77.39 GPa are in accordance with

2 experimental data: B=98 GPa [31] and C_{11}=166 GPa, C_{12}=64 GPa, C_{44}=79.6 GPa [32].

3   The electronic band structure calculations were performed for the LDA and HSE06 relaxed

4 structures of orthorhombic *Pbcm* and cubic silicon allotropes. As expected, the strong the band gap

5 value underestimation is found in the local density approximation for the cubic phase. Thus, one

6 may assume that LDA fails to threat the electronic structure of crystalline Si. On the contrary, the

7 good agreement is found in case of geometry optimization using the HSE06 method followed by the

8 electronic structure calculations using HSE06 also. The calculated E^i_g value for cubic silicon is in

9 excellent agreement with the experimental ones (1.12 eV [1,2,30.2]) obtained using the hybrid

10 functional HSE06 method for the structure optimized by the local density approximation. This fact

11 could be used as a good validation of the methods, and, hence, predicted values could be used as a

12 reference for the orthorhombic Si(oP32) allotrope. The calculated data obtained with different

13 approaches are shown in Table 2.

14 **Table 2**. Calculated indirect band gap values (in eV) for cubic and orthorhombic *Pbcm* silicon

15 allotropes

	Cubic			Orthorhombic *Pbcm*		
Functional for geom. opt.	LDA	LDA	HSE06	LDA	LDA	HSE06
Functional for band str. calc.	LDA	HSE06	HSE06	LDA	HSE06	HSE06
E^i_g (eV)	0.479	1.113	1.078	0.695	1.361	1.383

16

17   The electronic band structure of Si(oP32) calculated by the hybrid functional HSE06 method

18 for the LDA relaxed structure is plotted in Figure 3. For the energy band calculations, the high-

19 symmetry points of the BZ are selected as G–X–S–Y–G–Z–U–R–T–Z. The coordinates of the

20 special points of the Brillouin zone are: G(0,0,0), X(0.5,0,0), S(0.5,0.5,0), Y(0,0.5,0), Z(0,0,0.5),

21 U(0.5,0,0.5), R(0.5,0.5,0.5), T(0,0.5,0.5). It is found that the valence band (VBM) top is well

22 localized in the vicinity of the Γ-point in the center of the Brillouin zone. The conduction band

23 (CBM) bottom is located at X-point (0.5, 0, 0). The band gap value for the indirect electronic

transitions calculated within the hybrid functional HSE06 approach is equal to $E^i_g = 1.361$ eV. It is noteworthy to mention that the predicted Si(oP32) band gap value is very close to the theoretical value of Shockley–Queisser limit (1.34 eV) [33, 34]. Respectively, the Si(oP32) silicon modification seems to be a promising material for solar cells. The direct band gap is located at the Y-point of the Brillouin zone and the calculated band gap value is $E^d_g = 1.402$ eV. The results of quasi-particle G_0W_0 approximation are in agreement with the result of hybrid HSE06, and the difference between direct and indirect band gap values is insignificant, too (0.045 eV). However, there is a slight divergence in the band gap values of G_0W_0 approximation ($E^i_g = 1.127$ eV), with respect to HSE06 calculations ($E^i_g = 1.362$ eV), which is probably due to the fact that G_0W_0 was performed as "one-shot" calculations, while the calculations with the hybrid functional HSE06 approach were made as self-consisted. Thus, as a result of the electronic band structure analysis, we can conclude that Si(oP32) is a semiconductor material with indirect band gap $E^i_g = 1.362$ eV. The difference between direct and indirect band gaps is negligible.

The total and partial density of states of the Si(oP32) silicon allotrope structure obtained with the LDA method are shown in Figure 4. As a result of the curve analysis, one can find that the VBM and CBM are constructed mostly by the p-electrons of Si atoms, and s-electrons play a secondary role in the CBM formation.
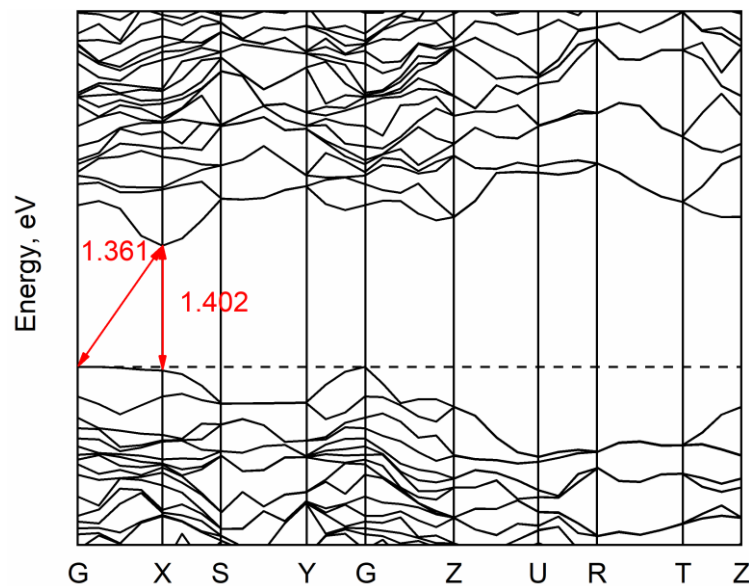
Figure 3. Electronic band structure of Si(oP32) silicon calculated with the use of HSE06.
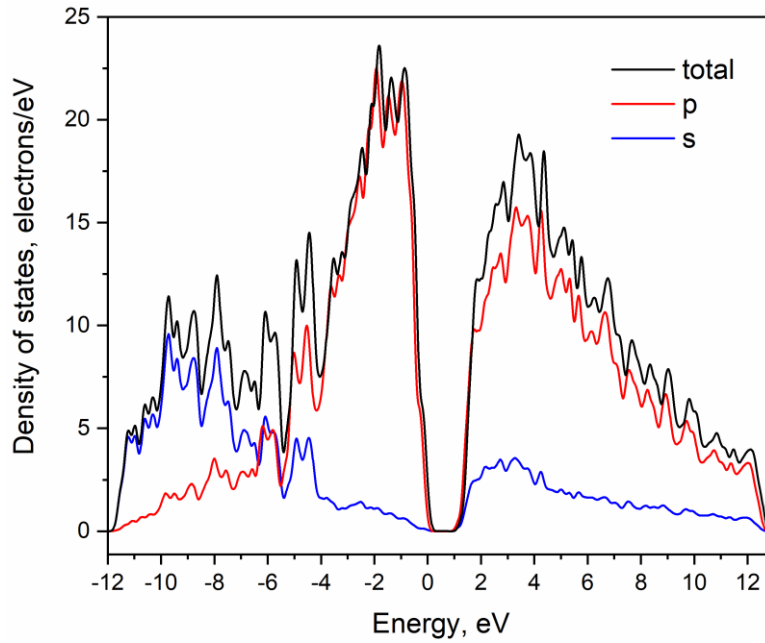
Figure 4. Total and partial density of states of Si(oP32).

The mechanical representation for the predicted Si(oP32) allotrope phase of Si (*Pbcm*) at the Brillouin zone center is $\Gamma_{vibr} = 13A_g + 10A_u + 14B_{1g} + 11B_{1u} + 11B_{2g} + 14B_{2u} + 10B_{3g} + 13B_{3u}$ [35] where the Raman active modes are $\Gamma_{Raman} = 13A_g + 14B_{1g} + 11B_{2g} + 10B_{3g}$, and the infrared active modes are $10B_{1u} + 13B_{2u} + 12B_{3u}$. The acoustic modes are $\Gamma_{Acoustic} = B_{1u} + B_{2u} + B_{3u}$. Thus, the Raman spectra of *Pbcm* silicon allotrope contain much more bands than that of cubic silicon. Cubic silicon has only one BZ center optical phonon mode active in the Raman spectrum at 522 cm^{-1} [36].

The calculated Raman spectrum of Si(oP32) allotrope is shown in Figure 5. The spectral line with the highest wavenumber value (533.6 cm^{-1}) is related to the stretching vibration of the shortest bond in the structure (Si1-Si3, see Fig. 6a) and, according to the calculation data, the stretching-like vibrations of different Si-Si pairs are located in the rage of 463–533 cm^{-1}. The various stretching-like and bending-like vibrations of structural units (Fig. 6b) are located in the range of 323–457 cm^{-1}. The weak band at 291.5 cm^{-1}, the most intensive band in the calculated Raman spectrum at 278.1 cm^{-1} and a very weak band at 196.1 cm^{-1} are related to the stretching of the structure as a whole, as shown in Fig. 6c, Fig. 6d, Fig. 6e correspondingly. The intense line at 129.0 cm^{-1} is a vibration of Si chains, as shown in Fig. 6f.

8
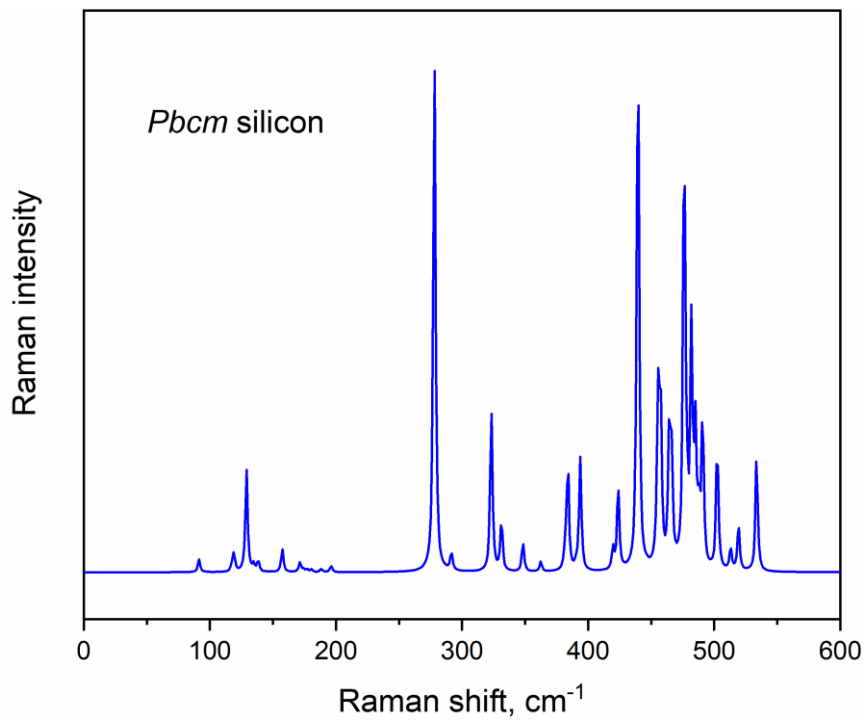
Figure 5. Calculated Raman spectrum of Si(oP32).
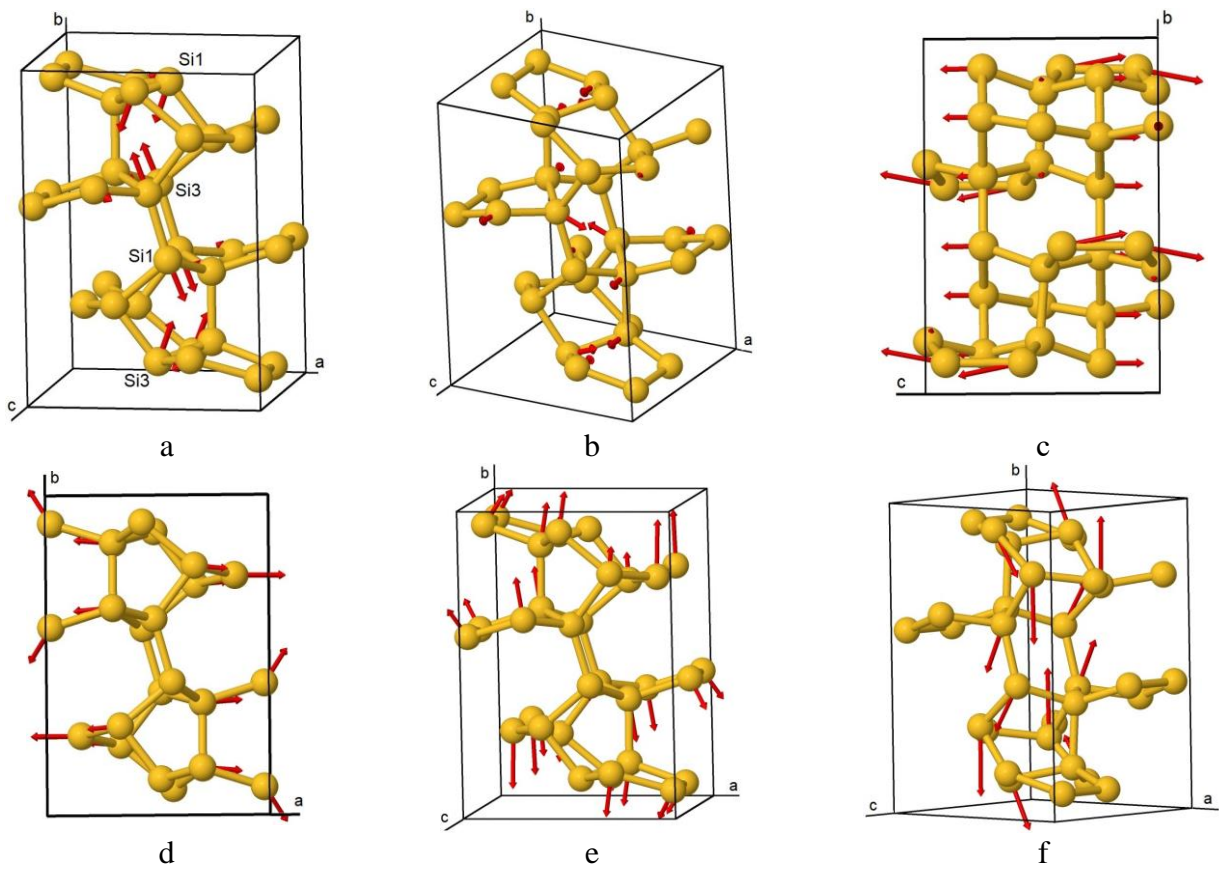
Figure 6. Displacements of Si(oP32) atoms in the vibrations with frequencies of 533.6 cm^{-1} (a), 446.7 cm^{-1} (b), 291.5 cm^{-1} (c), 278.1 cm^{-1} (d), 196.1 cm^{-1} (e) and 129.0 cm^{-1} (f).

It is worth noting that the orthorhombic Si(oP32) has the IR-active phonons, opposite to cubic silicon. The dynamical properties calculation was carried out and the simulated wavenumbers of Raman and Infrared active modes are listed in Table 3. The calculated phonon dispersion of Si(oP32) structure is shown in Figure 7. There are no phonon branches with imaginary frequencies, and, hence, the predicted structure should be stable with respect to phonon states.

Table 3. The calculated vibrational wavenumber values (cm^{-1}) of Si(oP32) allotrope

| №	Raman				Infrared			
	A_g	B_{1g}	B_{2g}	B_{3g}	A_u	B_{1u}	B_{2u}	B_{3u}
1	533.6	519.3	502.4	513.0	501.4	497.2	526.3	515.6
2	490.7	481.4	485.0	487.8	477.0	482.9	486.3	482.2
3	481.9	476.2	478.3	469.2	463.3	474.2	479.0	481.3
4	457.4	464.4	466.2	463.1	451.7	413.9	434.7	465.6
5	455.4	446.6	390.4	419.7	367.2	382.9	415.7	456.0
6	439.5	423.8	348.3	362.5	315.4	185.6	367.5	374.8
7	393.7	382.0	188.4	291.5	178.3	169.2	360.1	339.4
8	383.9	331.2	177.2	176.7	170.5	153.2	320.0	322.4
9	323.2	277.2	138.2	157.4	138.0	130.6	298.2	297.9
10	278.1	196.1	119.0	117.4	110.0	115.8	159.2	253.5
11	171.3	180.6	95.9				150.2	173.3
12	129.0	174.0					135.2	167.4
13	91.3	164.6					119.5	
14		134.7						
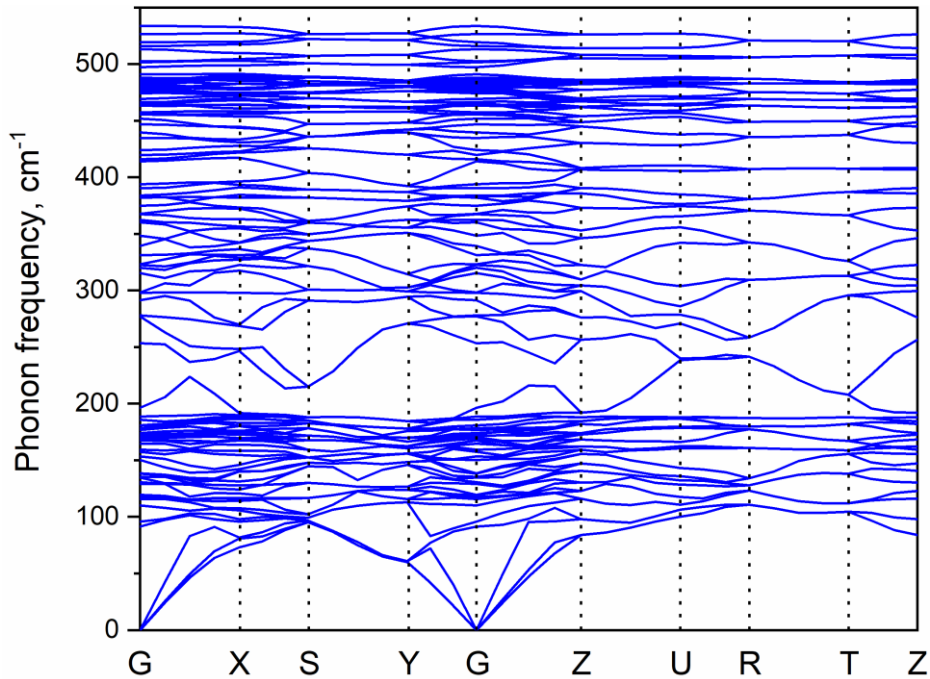
Figure 7. Calculated phonon dispersion curves of the Si(oP32) allotrope of silicon.

1   Earlier, other orthorhombic allotrope of silicon with the structure in space group *Cmcm* was

2   investigated [14]. In Fig. 8, the energy of the relaxed geometries of cubic and orthorhombic *Pbcm*

3   and *Cmcm* structures as a function of volume per formula unit is shown.
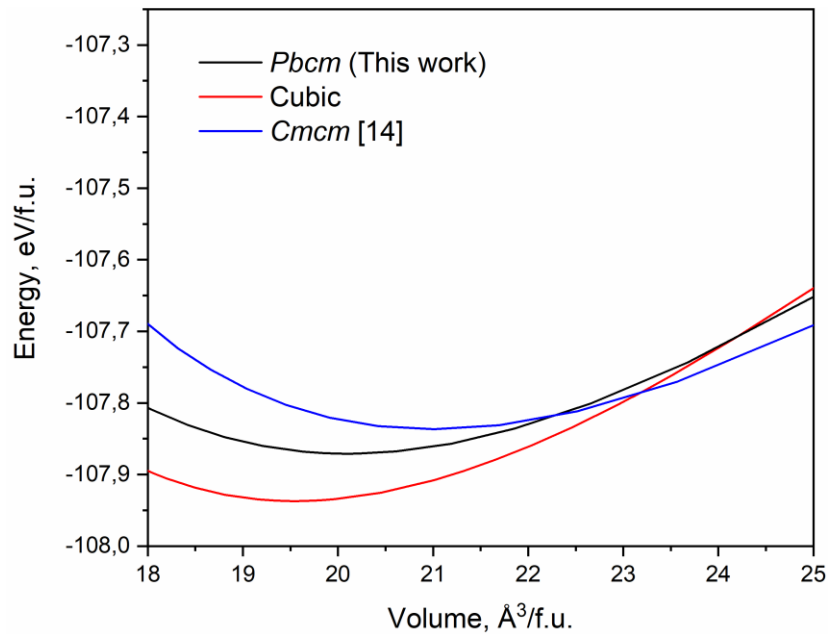
4

5   Fig. 8. Total energy per formula unit (f.u.) as a function of the volume per f.u. for cubic and

6   orthorhombic structures of silicon.

7   It is clearly seen that the phase transition from cubic to orthorhombic structures with *Cmcm*

8   and *Pbcm* spase groups may occur in the case of increasing the volume of per formula unit of cubic

9   silicon. These curves intersection points relate to the ~18.2 and ~23.8 percent increase of the cubic

10   silicon cell volume. As a possible way of such structure expansion, an intercalation of neutral atoms

11   into the cubic silicone structure may be considered. Herewith, the cubic structure still remains to be

12   stable, with respect to elastic stability conditions and phonon states. Thus, such possible phase

13   transitions should be of the first order type. As evident in Figure 8, the intersection of the energy per

14   volume curves for *Cmcm* and *Pbcm* phases exist and, thus, the structural transformation is possible

15   from Si_{24} to the Si(oP32) allotrope. Si_{24} (orthorhombic *Cmcm*) silicon was experimentally obtained

16   as a result of thermal `degassing' of Na_4Si_{24} at 400 K under dynamic vacuum [14]. Ge(oP32)

17   (orthorhombic *Pbcm*) germanium was experimentally prepared by the treatment of Li_7Ge_{12} in ionic

18   liquids [15]. The processes appropriate for the Li intercalation into cubic silicon are well known

and, supposedly, they could be developed to reach the Li_7Si_{12} phase [37-40]. Thus, it may be suggested that similar chemical reactions can also be designed for the formation of Si(oP32) modification. In terms of the total energy minimum, from results of our research follows that the total energy per formula unit for the Si(oP32) structure of orthorhombic silicon predicted in this work is lower than the one for *Cmcm* silicon. Thus, it can be reasonably assumed that the *Pbcm* phase is preferable than the *Cmcm* phase at ambient conditions.

4. Conclusions

In the present study, the unit cell parameters and atomic coordinates were predicted for a new anisotropic modification Si(oP32) of silicon. The Si(oP32) allotrope structure is similar to that of earlier synthesized germanium allotrope Ge(oP32). Respectively, because of chemical and structural similarities, the existence of continuous series of solid solutions Si(oP32)-Ge(oP32) can be assumed. The band gap value E_g = 1.361 eV predicted for Si(oP32) is very close to the Shockley–Queisser limit and it indicates that the silicon modification is a promising material for efficient solar cells. Thus, this is the time for the experimental synthesis of Si(oP32) allotrope and detailed exploration of their properties.

References

1. Y. Okada, Y. Tokumaru, Precise determination of lattice parameter and thermal expansion coefficient of silicon between 300 and 1500 K, J. Appl. Phys. 56 (2) (1984) 314-320.

2. A.G. Cullis, L.T. Canham, P.D. Calcott, The structural and luminescence properties of porous silicon, J. Appl. Phys. 82 (1997) 909-965.

3. . Kyozaburo Takeda, Kenji Shiraishi, Theoretical possibility of stage corrugation in Si and Ge analogs of graphite, Phys. Rev. B 50 (20) (1994) 14916-14922.

4. Gian G. Guzmán-Verri, L.C. Lew Yan Voon, Electronic structure of silicon-based nanostructures, Phys. Rev. B 76 (7) (2007) 075131.

5. Qianqian Wang, Bo Xu, Jian Sun, Hanyu Liu, Zhisheng Zhao, Dongli Yu, Changzeng Fan, Julong He, Direct band gap silicon allotropes, J. Am. Chem. Soc. 136 (28) (2014) 9826-9829.

6. Andrés Mujica, Chris J. Pickard, Richard J. Needs, Low-energy tetrahedral polymorphs of carbon, silicon, and germanium, Phys. Rev. B 91 (2015) 214104.

7. Antti J. Karttunen, Denis Usvyat, Martin Schütz, Lorenso Maschio, Dispersion interactions in silicon allotropes, Phys. Chem. Chem. Phys. 19 (11) (2017) 7699-7707.

8. Roxanne Tutchton, Christopher Marchbanks, Zhigang Wu, Structural impact on the eigenenergy renormalization for carbon and silicon allotropes and boron nitride polymorphs, Phys. Rev. B 97 (2018) 205104.

9.   Pei Zhang, Tao Ouyang, Chao Tang, Chaoyu He, Jin Li, Chunxiao Zhang, Ming Hu, Jianxin Zhong, Thermoelectric properties of four typical silicon allotropes, Modelling Simul. Mater. Sci. Eng. 26 (2018) 085006.

10. Menglei Hu, Ziao Wang, Yanheng Xu, Jiechun Liang, Jiagen Li, Xi Zhu, Fvs-Si48: a direct band gap silicon allotrope, Phys. Chem. Chem. Phys. 20 (2018) 26091-26097.

11. Qingyang Fan, Rui Niu, Wenzhu Zhang, Wei Zhang, Yingchun Ding, Sining Yun, t-Si$_{64}$: a novel Si allotrope, ChemPhysChem 20 (1) (2019) 128-133.

12. Patrick Vogt, Paola De Padova, Claudio Quaresima, Jose Avila, Emmanouil Frantzeskakis, Maria Carmen Asensio, Andrea Resta, Bénédicte Ealet, Guy Le Lay, Silicene: compelling experimental evidence for graphenelike two-dimensional silicon, Phys. Rev. Lett. 108 (2012) 155501.

13. Bianca Haberl, Malcolm Guthrie, Stanislav V. Sinogeikin, Guoyin Shen, James S. Williams, Jodie E. Bradby, Thermal evolution of the metastable r8 and bc8 polymorphs of silicon, High Press. Res. 35 (2) (2015) 99-116.

14. Duck Young Kim, Stevce Stefanoski, Oleksandr O. Kurakevych, Timothy A. Strobel, Synthesis of an open-framework allotrope of silicon, Nature Mat. 14 (2015) 169-173.

15. Zhongjia Tang, Alexander P. Litvinchuk, Melissa Gooch, Arnold M. Guloy, Narrow gap semiconducting germanium allotrope from the oxidation of a layered Zintl phase in ionic liquids, J. Am. Chem. Soc. 140 (22) (2018) 6785-6788.

16. S.J. Clark, M.D. Segall, C.J. Pickard, P.J. Hasnip, M.J. Probert, K. Refson, M.C. Payne, First principles methods using CASTEP, Z. Kristallogr. 220 (2005) 567-570. DOI: 10.1524/zkri.220.5.567.65075

17. J.P. Perdew and A. Zunger, Self-interaction correction to density-functional approximations for many-electron systems, Phys. Rev. B 23 (1981) 5048-5079. DOI: 10.1103/PhysRevB.23.5048

18. D.M. Ceperley and D.J. Alder, Ground state of the electron gas by a stochastic method, Phys. Rev. Lett. 45 (1980). 566-569. DOI: 10.1103/PhysRevLett.45.566

19. A.V. Krukau, O.A. Vydrov, A.F. Izmaylov, G.E. Scuseria, Influence of the exchange screening parameter on the performance of screened hybrid functionals, J. Chem. Phys. 125 (2006) 224106. DOI: 10.1063/1.2404663

20. H.J. Monkhorst and J.D. Pack, Special points for Brillouin-zone integrations, Phys. Rev. B 13 (1976) 5188-5192. DOI: 10.1103/PhysRevB.13.5188

21. D. Porezag, M. R. Pederson, Infrared intensities and Raman-scattering activities within density-functional theory, Phys. Rev. B 54 (11) (1996) 7830-7836. DOI: 10.1103/PhysRevB.54.7830

22. K. Refson, P.R. Tulip, S.J. Clark, Variational density-functional perturbation theory for dielectrics and lattice dynamics, Phys. Rev. B 73 (15) 155114. DOI: 10.1103/PhysRevB.73.155114.

23. S. Baroni, S. Gironcoli, A. D. Corso, P. Gianozzi, Phonons and related crystal properties from density-functional perturbation theory, Rev. Mod. Phys. 73 (2001) 515-562. DOI: 10.1103/RevModPhys.73.515

24. WilfriedG.Aulbur, Lars Jönsson, John W.Wilkins, Quasiparticle Calculations in Solids, Solid State Physics 54 (2000) 1-218.

25. X. Gonze, B. Amadon, P.-M. Anglade, J.-M. Beuken, F. Bottin, P. Boulanger, F. Bruneval, D. Caliste, R. Caracas, M. Côté, T. Deutsch, L. Genovese, Ph. Ghosez, M. Giantomassi, S. Goedecker, D.R. Hamann, P. Hermet, F. Jollet, G. Jomard, S. Leroux, M. Mancini, S. Mazevet, M.J.T. Oliveira, G. Onida, Y. Pouillon, T. Rangel, G.-M. Rignanese, D. Sangalli, R. Shaltaf, M. Torrent, M.J. Verstraete, G. Zerah, J.W. Zwanziger, ABINIT: First-principles approach to material and nanosystem properties, Comput. Phys. Commun. 180 (2009) 2582–2615.

26. Xavier Gonze, Gian-Marco Rignanese, MatthieuVerstraete, Jean-Michel Beuken, Yann Pouillon, Razvan Caracas, Francois Jollet, Marc Torrent, Gilles Zerah, Masayoshi Mikami, Philippe Ghosez, Marek Veithen, Jean-Yves Raty, Valerio Olevano, Fabien Bruneval, Lucia Reining, Rex Godby, Giovanni Onida, Donald R. Hamann and Douglas C. Allan, A brief introduction to the ABINIT software package, Z. Kristallogr. Cryst. Mater. 220 (2005) 558–562.

27. S. Lebègue, B. Arnaud, M. Alouani, and P. E. Bloechl, Implementation of an All-electron GW Approximation Based on the Projector Augmented Wave Method without Plasmon Pole Approximation: Application to Si, SiC, AlAs, InAs, NaH, and KH, Phys. Rev. B 67 (2003) 155208.

28. M. Born, On the stability of crystal lattices, I. Math. Proc. Cambridge, 36 (2) (1940) 160-172. DOI: 10.1017/S0305004100017138

29. M. Born and K. Huang, Dynamics theory of crystal lattices, Oxford University Press, Oxford, UK, 1954.

30. F. Mouhat and F.-X. Coudert, Necessary and sufficient elastic stability conditions in various crystal systems, Phys. Rev. B 90 (22) (2014) 224104. DOI: PhysRevB.90.224104

31. O. Madelung, U. Rössler, M. Schulz, Silicon (eds.) (Si) Young's modulus, torsion modulus, bulk modulus (various structures). In Group IV Elements, IV-IV and III-V Compounds. Part a -

Lattice Properties. Landolt-Börnstein - Group III Condensed Matter (2001) Springer, Berlin, Heidelberg. DOI: 10.1007/10551045_217

32. O. Madelung, U. Rössler, M. Schulz, Silicon (eds.) Silicon (Si) elastic moduli of Si-I. In Group IV Elements, IV-IV and III-V Compounds. Part a - Lattice Properties. Landolt-Börnstein - Group III Condensed Matter (2001) Springer, Berlin, Heidelberg. DOI: 10.1007/10551045_212

33. W. Shockley &H.J. Queisser. Detailed balance limit of efficiency of pn junction solar cells. J. Appl. Phys. 32 (1961) 510–519. DOI: 10.1063/1.1736034

34. S. Rühle, Tabulated values of the Shockley–Queisser limit for single junction solar cells, Solar Energy, 130 (2016) 139-147. DOI: 10.1016/j.solener.2016.02.015

35. E. Kroumova, M.I. Aroyo, J.M. Perez-Mato, A. Kirov, C. Capillas, S. Ivantchev, H. Wondraschek, Bilbao Crystallographic Server : Useful databases and tools for phase-transition studies, Phase Transit. 76 (2003), 155-170. DOI: 10.1080/0141159031000076110

36. H. Richter, Z.P. Wang, L. Ley, The one phonon Raman spectrum in microcrystalline silicon, Solid State Commun. 39 (1981) 625-629. DOI: 10.1016/0038-1098(81)90337-9

37. C. J. Wen, R. A. Huggins, Chemical diffusion in intermediate phases in the lithium-silicon system, J. Solid State Chem. 37 (3) (1981) 271-278.

38. M. N. Obrovac and L. Christensen, Structural changes in silicon anodes during lithium insertion/extraction, Electrochem Solid St. 7 (5) (2004) A93-A96. DOI: 10.1149/1.1652421

39. J. Li and J. R. Dahn, An in situ X-ray diffraction study of the reaction of Li with crystalline Si, J. Electrochem Soc. 154 (3) (2007) A156-A161. DOI: 10.1149/1.2409862

40. V. L. Chevrier, J. W. Zwanziger, J. R. Dahn, First principles study of Li–Si crystalline phases: Charge transfer, electronic structure, and lattice vibrations, J. Alloy Compd. 496 (2010) 25-36. DOI: 10.1016/j.jallcom.2010.01.142